FLUID DYNAMIC EFFECTS IN THE FUEL ELEMENT TOP NOZZLE AREA DURING REFILLING AND REFLOODING

BY

A.Hawighorst, H. Kröning, F. Mayinger

Institut für Verfahrenstechnik
der Universität Hannover
Federal Republic of Germany

ABSTRACT

At an unheated 4x4 rod bundle air/water test facility optical investigations of the entrainment behavior and counter current flow experiments were performed with a large variety of test conditions:

- flow duct geometry
- internals (tie-plate, bundle length, number of grid spacers, rod diameter)
- type of injection (different nozzles, porous sinter metal)
- different mass flux for air and water

In addition several flooding models were compared with the own experimental data.

In conclusion it was found that the type of injection has only a weak influence whereas the geometrical conditions upstream of the narrowest flow area (presence of bundle, grid spacer) have an important effect on the flooding behavior. In addition a comparison of the applicability of different flooding models shows that only the models based on dimensionless numbers expressed by superficial velocities, show a good agreement with the own experimental data.

INTRODUCTION

Countercurrent flow of a gas and a liquid occurs during emergency core cooling conditions in the region of the downcomer and the core. In the FRG-PWR, two separate emergency core cooling systems are provided which reflood the core, the top injection (hot leg injection) and the bottom injection (cold leg injection).

From the top injection the water must pass through the upper plenum and the end-box into the core region. Furthermore steam will be generated from the bottom and the top ECCS water and this steam will flow upward through the core and into the upper plenum region. The action of steam flowing upwards while coolant water flows downward can lead to a condition defined as countercurrent flow limiting (CCFL), which tends to restrict the water down flow.

Furthermore water droplets will be entrained at the bottom and at the top quench front by sputtering and a part of these droplets is transported by the steam flow through the core and deentrains in the upper plenum region. This deentrained water and the upwards flowing steam can lead to the same fluid dynamic behavior discussed before.

The purpose of this paper is to discuss the influence of flow restrictions, like the tie-plate and the grid spacers, onto the countercurrent flow limitation.

For these experiments an air-water test device with a 4x4 unheated rod bundle, representing 1/16 th of the upper part of a FRG-PWR fuel-element was constructed, shown in Fig. 1.

DESCRIPTION OF THE TEST SET-UP

The test set-up (Fig. 1) consists of an air loop, one water loop for bottom injection and, another water loop for top injection. The test vessel includes the flow duct of square cross section with the 4x4 unheated rod bundle, 3 grid spacers, the tie-plate and the injection device for CCF-experiments. The inlet mass flows are measured by flow element flow meters with different ranges and the outlet water mass flow - fall back and carry over - are measured by collecting tanks.

Fig. 2 gives informations about the internals of the square flow duct. The injection device which injects water through porous sinter metal walls into the flow duct is located 200 mm above the tie-plate. The thickness of the tie-plate is 20 mm and the hole diameters are d=10.5 mm for the 59x59 mm flow duct and d= 10.0 mm for the 57x57 mm flow duct.

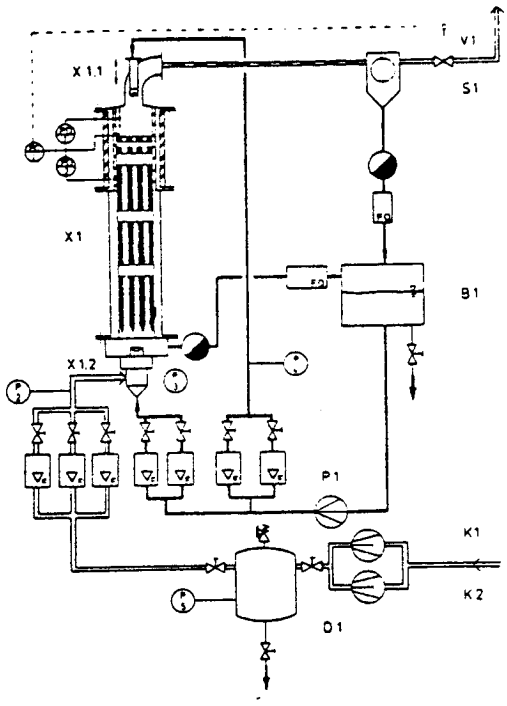

X1 Test vessel with a 4×4 rod bundle flow duct
X1.1 Top injection nozzle
X1.2 Bottom two-phase injection nozzle
V1 Pressure controlling system (valve)
S1 Twist separator
B1 Water store tank
K1,K2 Piston compressors
D1 Pressure vessel
P1 Centrifugal pump

FIG. 1 AIR/WATER TEST SET UP

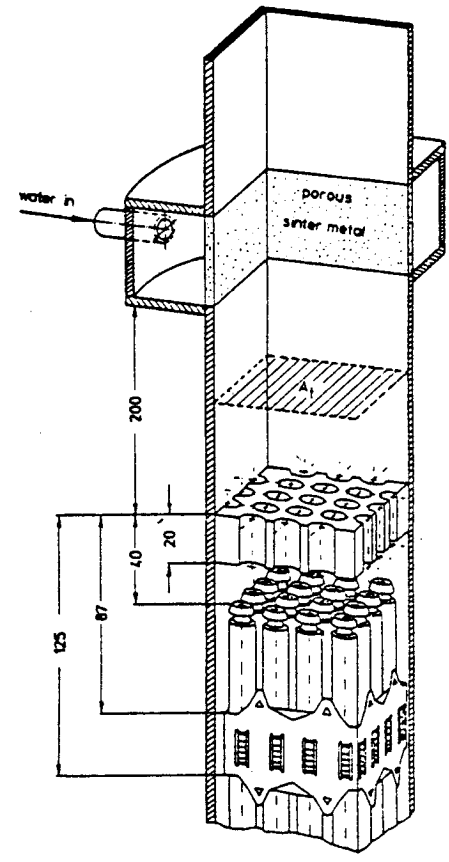

FIG. 2 FLOW DUCT WITH INTERNALS AND WATER INJECTION DEVICE

The 16 rods are fixed by 1 or 3 original KWU grid spacers,dependent on the bundle lenght.

For the entrainmment investigations at countercurrent flow conditions an optical investigation device was developed and constructed, shown in Fig. 3. In general, at two-phase flows in a flow duct the shroud walls are wetted by a liquid film. This liquid film prevents the radial photography of the entrained droplets in the gas core.

The weir elements through which the parallel light passes turnes round the liquid film. Droplets, which enter the seperating volume and wet the windows, are removed by a small air jet and drained.

In the case of co-corrent flow the water is injected in the bottom part of the test channel by a two-phase nozzle, therefore the porous sinter section can be used to suck off the above mentioned upclimbing liquid film.The photographs which we got from this optical arrangement,working with a parallel light technique, are shadow photographs.

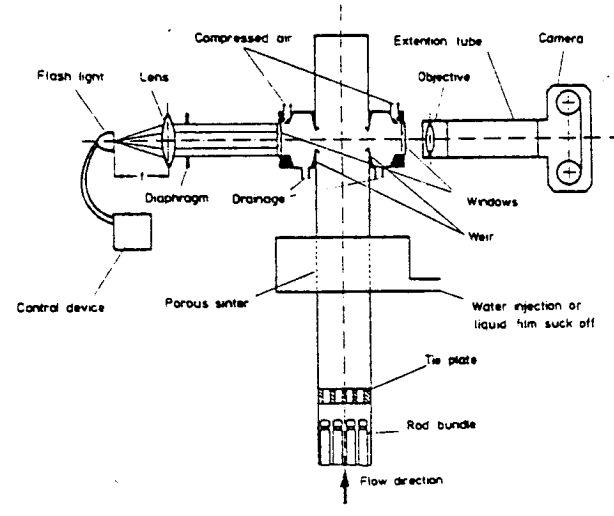

FIG. 3 TEST DEVICE FOR ENTRAINMENT PHOTOGRAPHS

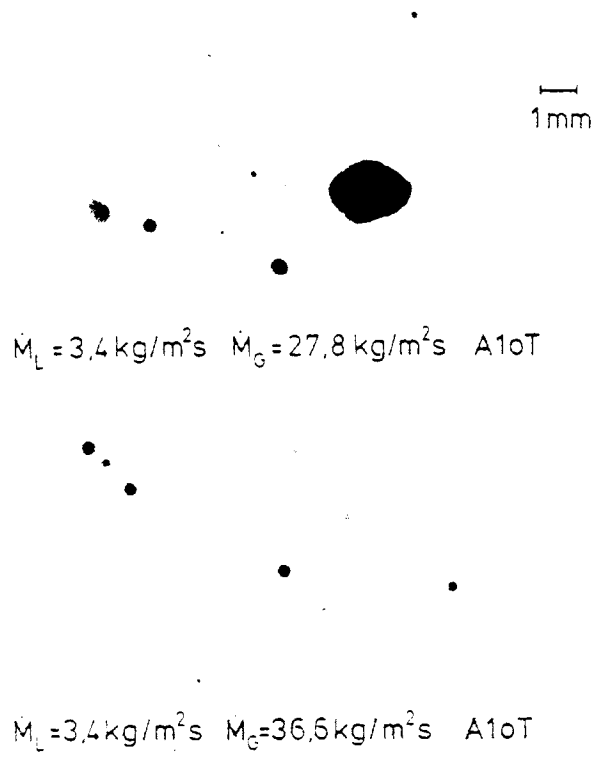

FIG. 4 ENTRAINMENT PHOTOGRAPHS

OPTICAL INVESTIGATIONS

Fig. 4 shows typical examples of droplets entrained at co-current conditions. The air and water mass fluxes were varied in a large range. These entrainment photographs show that an increasing water mass flux at constant air mass flux leads to droplets which become larger in size whereas at constant water mass flux and increasing air mass flux the drop size becomes smaller.

For the evaluation of the droplet photographs an automatic image analysing system is developed by us. The image will be digitized by a scanner into discrete pixels with 256 different grey levels and the sharp droplets can be detected by a computer program on the basis of differential operations.

A practicable method of representing size distributions is the cumulative distribution plot, formed by plotting the cumulative probability percentage of droplets greater or less than a given size, against the size.

Fig. 5 shows results of drop size investigations, Fig. 5a shows the droplet distribution for a constant liquid flux and different air fluxes and Fig. 5b for a constant air flux and different liquid fluxes. These figures confirm the conclusions which were illustrated by the photographs, namely a decreasing in drop size with increasing air mass flux and with decreasing water mass flux.

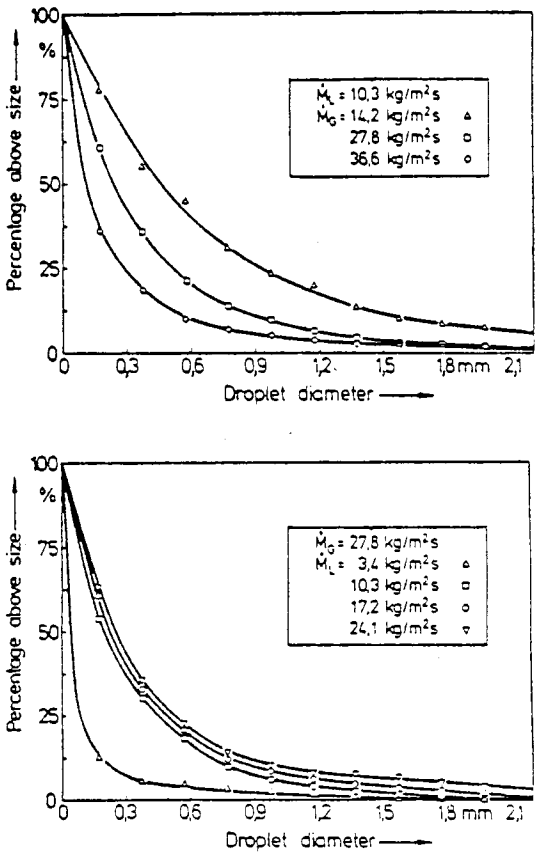

FIG. 5 DROPLET SIZE DISTRIBUTIONS
A) FOR CONSTANT LIQUID FLUX AND DIFFERENT AIR FLUX
B) FOR CONSTANT AIR FLUX AND DIFFERENT LIQUID FLUX

The curves are shown in this diagram were gained by a smoothing calculation. The curves represent a logarithmic distribution which is based on the following expression with x-drop diameter and a,b -parameters:

$$F(x) = 1 - \frac{1}{b\sqrt{2\pi}} \int e^{-\frac{1}{2}\left(\frac{\ln x - a}{b}\right)^2} dx \qquad (1)$$

A comparison of droplet size distributions gained from our own single tube tests /1,2/ and tests from other authors /3,4/ with results gained from our own bundle tests (Fig.6) shows, that under identical mass flux conditions the drops become greater in size with bundle tests. In the case of single tube tests the droplets are generated by undercutting of disturbance waves or by breakdown (rolling) of disturbance waves /4/.

This droplet generation mechanism leads to very small droplets whereas the droplet generation mechanism at the top of the rods, the break off of the upwards flowing liquid film from the rods and the sputtering mecha-

nism on the cross pieces of the tie-plate yields to larger droplets at this mass flux conditions.

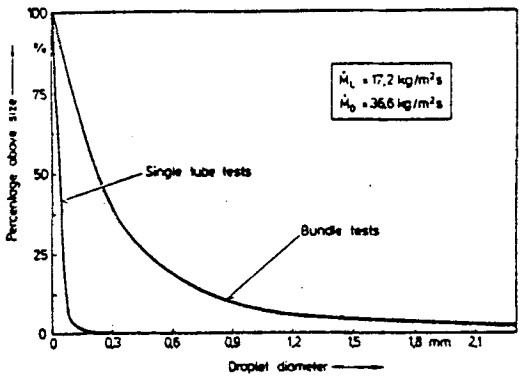

FIG. 6 COMPARISON BETWEEN BUNDLE TEST AND SINGLE TUBE TEST RESULTS

Fig. 7 shows a typical example of the droplets formation at the edges of the tie-plate holes. At co-current conditions an upwards climbing liquid film is breaking off at the edges of the holes and droplets are be formed. During countercurrent flow conditions a small liquid layer is weeping at the cross pieces between the holes and a partial blockage of the holes by liquid takes place. This liquid is blown out in the form of droplets. Depen-dending on the diameter and the gas velocity these droplets are carried over or fall back.

The formation of a splashing regime is shown in Fig. 8. The upper part of this figure shows photographs of different flow situations dependending on the air superficial velocity. At the onset of flooding we can observe a rapidly growing of the droplet splashing regime. In the bottom part of this figure the ratio of the carried over water to the total injected water is shown as a function of the air velocity. Furthermore the flow conditions are indicated at which the photographs were taken. The onset of carry over depends on the maximum countercurrent water which can penetrate at this air flux. A detailed discussion is given in the next chapter.

COMPARISON OF SEVERAL DIFFERENT FLOODING MODELS

In the past a lot of flooding models were presented in the literature. In general we can distinguish between four models which are basing on

o dimensionless numbers formed by superficial velocities

$$\overset{*}{j}_l = f\left(c, \overset{*}{j}_g\right)$$

proposed by:
Wallis /5/, Kutateladze /6/, Bankoff /7/, Feind/8/, Alekseev /9/, Susuki /10/, Grolms /11/

FIG. 7 SPLASHING MECHANISM AT THE TIE-PLATE

o separated film flow models

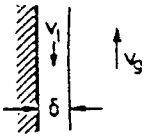

proposed by:
Dukler /12/, Taitel et al /13/

o instability models of surface waves

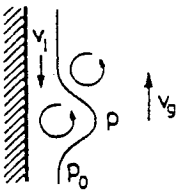

proposed by:
Sherer et al /14/, Centinbudakler /15/, Imura /16/, Richter /17/, Zvirin and Duffey /18/

o perforated plate weeping models

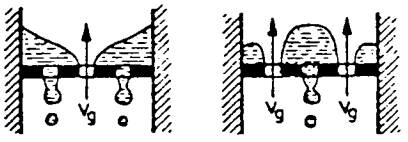

proposed by:
Wallis et al /19/, Naitoh /20/, Liu /21/

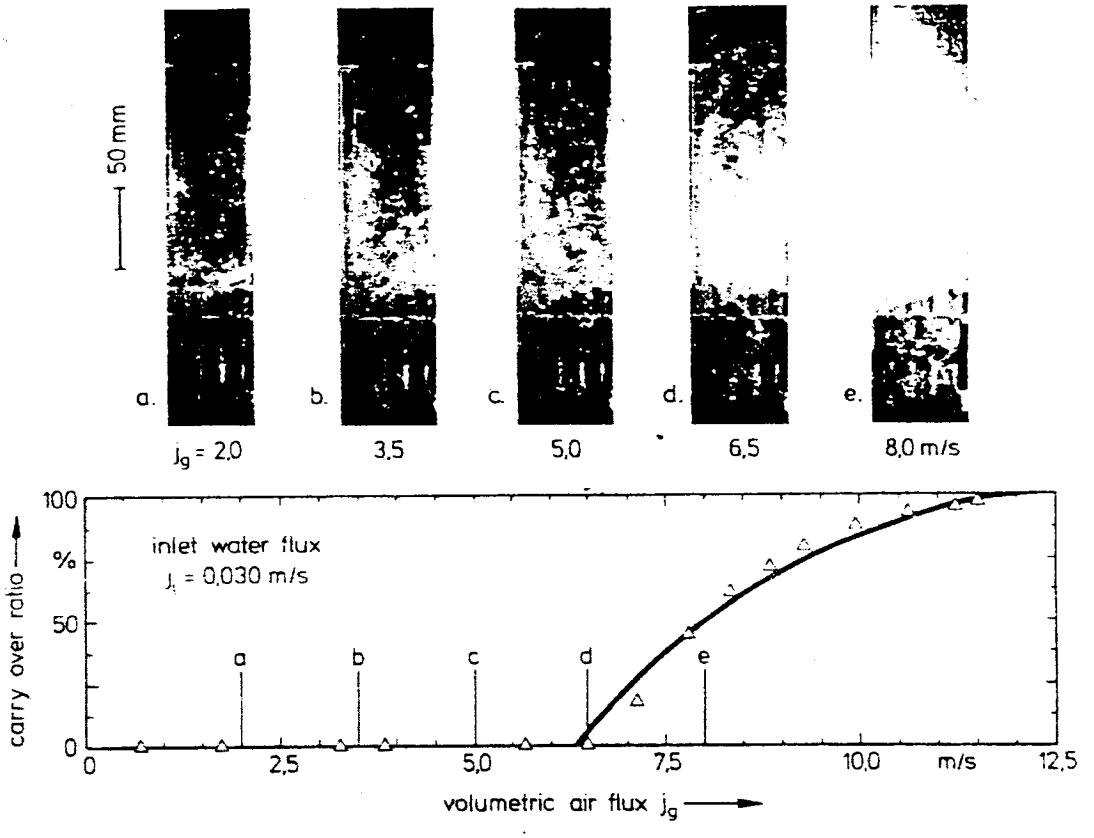

FIG: 8 FORMATION OF A SPLASHING REGION AT FLOODING CONDITIONS

A comparison of our own experimental rod bundle flooding data with several different flooding models is shown in Fig. 9 where the superficial velocity of the countercurrent water are cross plotted to the air superficial velocity. This comparison shows a nonuniform behavior of the several models, only the models of Wallis, Kutateladze and Bankoff, which based on dimensionless numbers formed by superficial velocities, show a good agreement with the experimental data. In the following these three models will be discussed.

The Wallis correlation is given by:

$$J_g^{*1/2} + m J_l^{*1/2} = C$$

$$J_g^{*} = j_g \cdot \rho_g^{1/2} [g \cdot D(\rho_l - \rho_g)]^{-1/2}$$

$$J_l^{*} = j_l \cdot \rho_l^{1/2} [g \cdot D(\rho_l - \rho_g)]^{-1/2}$$

D characteristic length

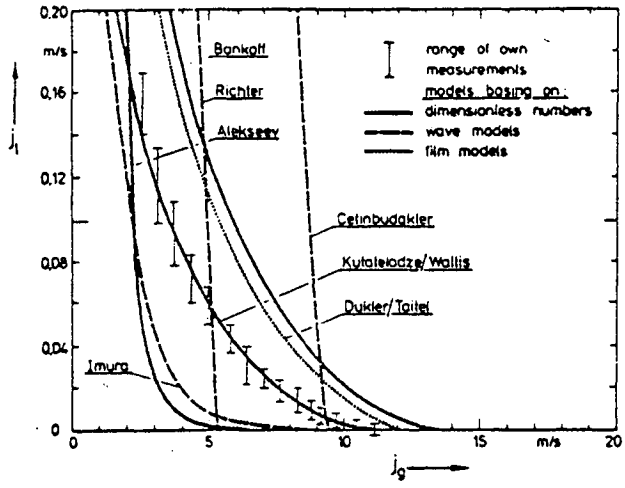

FIG: 9 COMPARISON OF SEVERAL FLOODING MODELS

In the case of bundle experiments it is very problematic to determine the characteristic lenght D, especially if the influence of geometrical conditions on the flooding behavior shall be studied and discussed. For that the nondimensional velocities model proposed by Kutateladze is a useful way.

If the characteristic length of the Wallis correlation will be substituted by the Laplace constant

$$LP = [\sigma / g(\rho_l - \rho_g)]^{1/2} \qquad (5)$$

the Wallis correlation changes to the Kutateladze correlation.

$$K_g^{1/2} + M K_l^{1/2} = N \qquad (6)$$

$$K_g = j_g \cdot \rho_g^{1/2} [g \cdot \sigma (\rho_l - \rho_g)]^{-1/4} \qquad (7)$$

$$K_l = j_l \cdot \rho_l^{1/2} [g \cdot \sigma (\rho_l - \rho_g)]^{-1/4} \qquad (8)$$

For perforated plates Bankoff et al have introduced a new modified Wallis correlation, Eq. (9), which interpolates between the characteristic length D (a geometrical length) and the Laplace diameter LP, which is influenced by thermodynamic properties.

$$H_g^{*1/2} + H_l^{*1/2} = C \qquad (9)$$

$$H_g^* = j_g [\rho_g]^{1/2} \cdot [g w (\rho_l - \rho_g)]^{-1/2} \qquad (10)$$

and

$$H_l^* = j_l [\rho_l]^{1/2} \cdot [g w (\rho_l - \rho_g)]^{-1/2} \qquad (11)$$

where the interpolative length scale is

$$w = D^{1-\beta} \cdot LP^{\beta} \qquad 0 \leq \beta \leq 1 \qquad (12)$$

if ß becomes 0, H^* becomes equal to J^* and if ß becomes 1, H^* becomes equal to K.

The parameter ß can be expressed by the following function

$$\beta = \tanh(\gamma k_c D) \qquad (13)$$

where the critical wave number $k_c = 2\pi/tp$ corresponds to the maximum wavelength which can be sustained on an interface of lenght tp, the plate thickness and γ the perforation ratio, is the fraction of the plate area occupied by holes.

For the constant C the following equations are given:

$$C = 1.07 + 4.33 \times 10^{-3} Bo \qquad Bo < 200 \qquad (14)$$

$$C = 2 \qquad Bo > 200 \qquad (15)$$

where the Bond number Bo is defined as

$$Bo = n \pi D [g(\rho_l - \rho_g)/\sigma]^{1/2} \qquad (16)$$

with n as the number of holes.

A comparison of the Bankoff H^* - model and the Kutateladze K-model with our own experimental data has shown, that the K-curve gives a better agreement with the experimental data. The data for this comparison gained from tests, at which only the tie-plate was installed in the test channel - at similar experimental conditions, at which the H^* - model was developed by Bankoff.

The Wallis-correlation and the Kutateladze correlation are identical in this case, because the tests are performed at constant thermodynamic conditions and consequently the Laplace diameter is constant.

Therefore in the next chapter only the Kutateladze-correlation will be discussed.

THE CARRY OVER RATIO DIAGRAM

Fig. 10 describes the ratio of the carried over water to the total injected water vs. the air mass flow and the influence of the total injected water mass flow rate on the ratio of the carried over water.

The experimental results show that at constant injected water flux and increasing air superficial velocitiy the carried over water ratio increased from 0 % up to 100 %. The onset of carry over depends on the maximum coutercurrent water which can penetrate at this air-velocity into tne bottom plenum. At an air velocity of about 12 m/s all injected water is carried over.

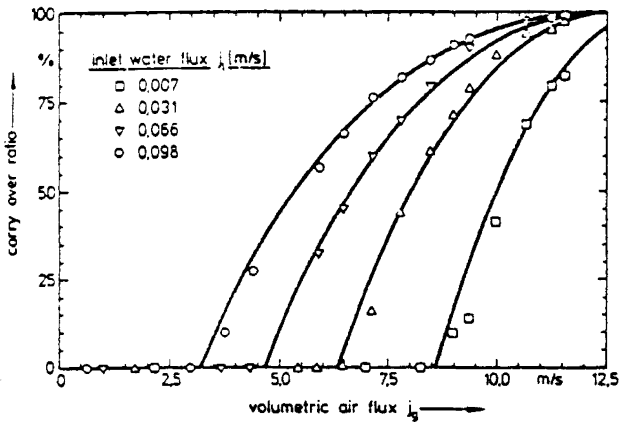

FIG: 10 INFLUENCE OF THE VOLUMETRIC AIR FLUX ON THE CARRY-OVER RATIO

The curves plotted in this diagram are gained from a computer correlation on the basis of the mass balance

$$j_{lt} = j_l - j_{lb} \qquad (17)$$

or

$$\frac{j_{lt}}{j_l} = 1 - \frac{j_{lb}}{j_l} \qquad (18)$$

and the Kutateladze equation.

From the Kutateladze correlation we get the relation between the CCF-water superficial velocity j_{lb} and the air superficial velocity j_g

$$j_{lb} = \left(\frac{N}{M} \sqrt{[g\sigma(\varrho_l - \varrho_g)/\varrho_l^2]^{1/4}} - \frac{1}{M} \sqrt{j_g (\varrho_g/\varrho_l)^{1/2}} \right)^2 \qquad (19)$$

the constants N and M are correlated from the experimental data by the least squares method.

With the expressions (18) and (19) the carry over ratio becomes

$$\frac{j_{lt}}{j_l} = 1 - \frac{1}{j_l} \left(\frac{N}{M} \sqrt{[g\sigma(\varrho_l - \varrho_g)/\varrho_l^2]^{1/4}} - \frac{1}{M} \sqrt{j_g (\varrho_g/\varrho_l)^{1/2}} \right)^2 \qquad (20)$$

For these geometrical conditions the constants are determined to N = 1.94 and M = 1.14 and the calculated curves show a good agreement with the experimental results.

INFLUENCE OF LIQUID INJECTION AND FLOW DUCT GEOMETRY ON THE FLOODING CONDITIONS

For single tube tests a strong influence of the water inlet conditions on the flooding behavior were found by different authors e.g. Feind /8/, Wallis /5/, Imura /16/.

To get an idea how the type of injection and the geometrical conditions are influencing the own bundle experiments, a large variety of test-conditions were used. Table 1 shows the test matrix and Fig. 11 the influence of different internals on the relative free flow area.

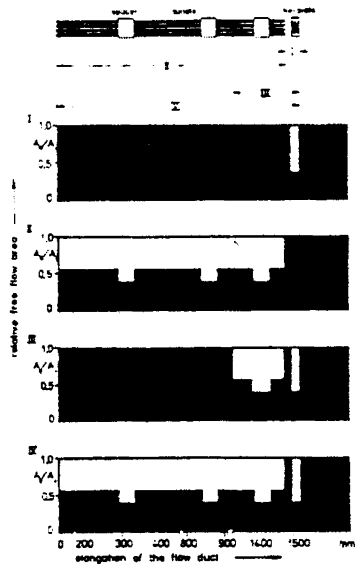

Fig. 11 COMPARISON OF THE RELATIVE FREE FLOW AREAS AT DIFFERENT TEST CONDITIONS

In Fig. 12 a comparison is plotted of tests at which the water was injected through porous sinter metal walls into the flow duct and tests at which the water was injected by nozzles. In both cases the injection level was located 200 mm above the tie-plate at which the nozzles were arranged in the center of the flow duct.

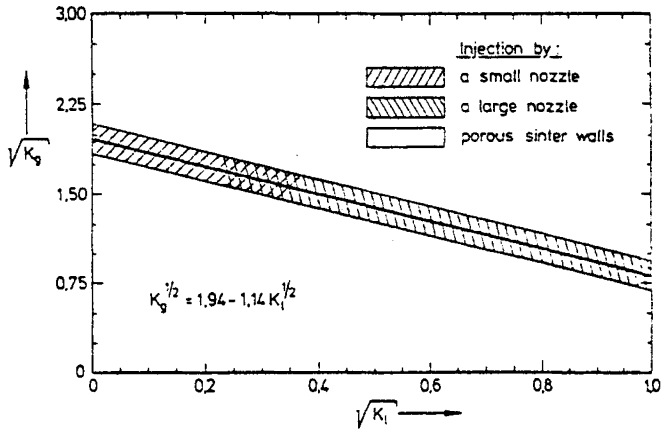

Fig. 12 INFLUENCE OF DIFFERENT WATER INJECTION DEVICES ON THE FLOODING BEHAVIOR

Test No	Type of water injection	Channel geometries	Internals	
111101	water injection by porous sinter metal	59×59 mm square flow duct	1500 mm rod bundel with 3 spacer and tie-plate rod diameter 10 mm	
111103			only tie-plate	
111105			150 mm rod bundel with 1 spacer and tie-plate rod diameter 10 mm	
111107			1500 mm rod bundel with 3 spacer and tie-plate rod diameter 10,8 mm	
111109			150 mm rod bundel with 1 spacer and tie-plate rod diameter 10,8 mm	
111201		57×57 mm square flow duct	1500 mm rod bundel with 3 spacer rod diameter 10 mm	with tie-plate
111202				no tie-plate
131201	by a small nozzle			with tie-plate
141201	by a large nozzle			with tie-plate
141202				no tie-plate

TAB 1 TEST MATRIX FOR THE AIR/WATER COUNTER-CURRENT FLOW EXPERIMENTS

The comparison of experimental results of these test series shows that all test data are well represented by one flooding curve i.e. at these test conditions the flooding curve is not influenced by the type of injection.

Furthermore the experiments resulted that tests at which a short bundle (150 mm with one spacer) had been installed are well represented by the same flooding curve.

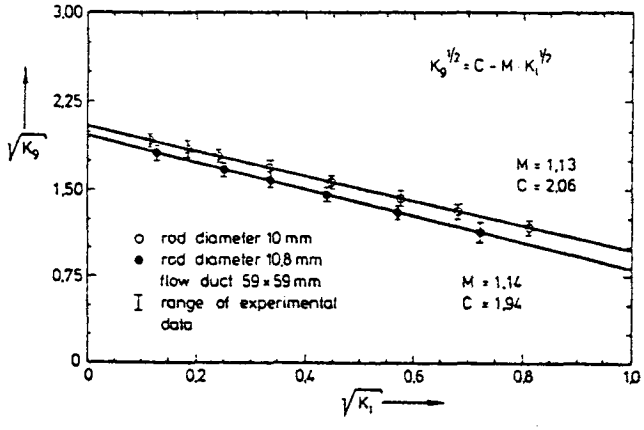

FIG 13 INFLUENCE OF THE ROD DIAMETER ON THE FLOODING BEHAVIOR

Experiments at which the rod diameter of the bundle was varied, are described in Fig.13. At constant flow duct geometry a change of the rod diameter leads to different flooding curves in the Kutateladze-diagram. It means the constants of the Kutateladze-correlation depend on the relative free flow area and obtain other values. Because of the small change of the geometry we can observe only a weak influence on the flooding curve.

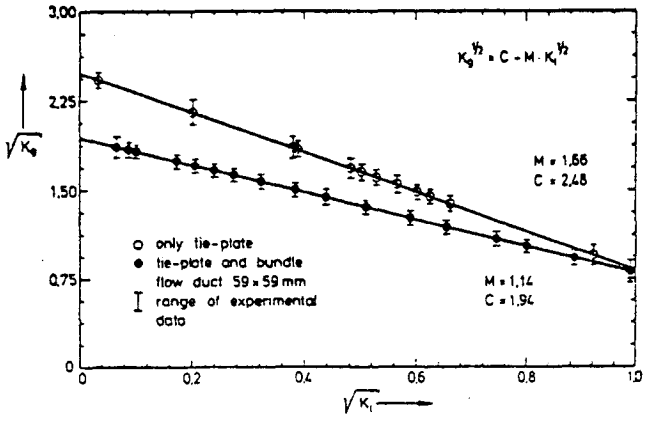

FIG. 14 INFLUENCE OF THE BUNDLE PRESENCE ON THE FLOODING BEHAVIOR

Fig. 14 and 15 show a comparison of tests at which only a tie-plate was installed in the flow duct and tests at which a rod bundle was arranged upstream the tie-plate. These two figures, Fig. 14 and 15, illustrate clearly the strong influence of the rod bundle on the flooding behavior and the importance of the correctly simulated flow conditions upstream the narrowest flow area for the determination of flooding curves, especially if these experiments shall contribute to an improvement of LOCA/ECCS-computer codes.

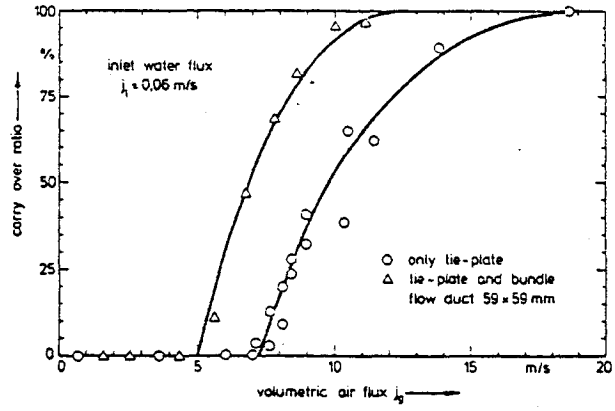

FIG. 15 INFLUENCE OF THE BUNDLE PRESENCE ON THE CARRY-OVER RATIO

Fig. 15 makes evident the importance of the bundle presence. At a volumetric air flux of 7 m/s all water is penetrating through the perforated plate, if only the tie-plate is installed, whereas at flow conditions at which the bundle is installed too, 60 % of the injected water is carried over.

LIST OF SYMBOLS

A_b	blocked cross section of the flow duct
A_o	free cross section of the flow duct
A_t	total cross section of the flow duct
c	Wallis parameter
C	Bankoff parameter
D	diameter
g	gravity constant
j	superficial velocity
K	wave number
m	Wallis paramter
M	Kutateladze parameter
N	Kutateladze parameter
ϱ	density
σ	surface tension
β	Bankoff paramter
γ	perforation ratio

SUBSCRIPTS

g	gas
l	liqiud
lt	carry over liquid
tb	drain (CCF-)' liquid

DIMENSIONLESS GROUPS

Bo	Bond number
Fr	Froude number

$$J_l^* \qquad j_l \cdot \varrho_l^{1/2} [g \cdot D(\varrho_l - \varrho_g)]^{-1/2}$$

$$J_g^* \qquad j_g \cdot \varrho_g^{1/2} [g \cdot D(\varrho_l - \varrho_g)]^{-1/2}$$

$$K_l \qquad j_l \cdot \varrho_l^{1/2} [g \cdot \sigma(\varrho_l - \varrho_g)]^{-1/4}$$

$$K_g \qquad j_g \cdot \varrho_g^{1/2} [g \cdot \sigma(\varrho_l - \varrho_g)]^{-1/4}$$

LITERATURE

/1/ Mayinger, Kröning, Hawighorst
Fluiddynamische Effekte im Brennelementkopfbereich während des Wiederauffüllens und Flutens
BMFT-Forschungsbericht 150366

/2/ Langner,
Untersuchungen des Entrainment-Verhaltens in stationären und transienten zweiphasigen Ringströmungen,
Dissertation T.U. Hannover, 1978

/3/ Ghazanfari,
Experimentelle Untersuchungen des Wärmeübergangs in einer Tropfenströmung nach Überschreiten der Benetzungstemperatur
Dissertation, T.U. Bochum, 1977

/4/ Hewitt, Hall-Taylor,
Annular Two-Phase Flow,
Pergamon Press, 1970

/5/ Wallis, G.B.
Flooding velocities for air and water in vertical tubes,
UKAEA AEEW R-123, 1961

/6/ Kutateladze, S.S., Sorokin, Yu.L.,
The hydrodynamic stability of vapor-liquid systems, in
Problems of heart transfer and hydraulics of two-phase media,
Verlag Pergamon Press, Ocford

/7/ Bankoff, S.G., Tankin, R.S., Yaen, M.C., Hsieh, C.L.,
Countercurrent flow of air/water and steam/water through a horizontal perforated plate,
Int. Journal Heat Mass Transfer Vol. 24 No. 8 pp 1381-1395, 1981

/8/ Feind, K.,
Strömungsuntersuchungen bei Gegenstrom von Rieselfilmen und Gas in lotrechten Rohren,
VDI-Forschungsheft 481, 196o

/9/ Alekseev. A.E., Poberezkin, A.E., Gerasimov, P.V.,
Determination of Flooding rates in Regular Packings,
Heat Transfer - Soviet Research Vol. 4 No. 6, 1972

/10/ Suzuki, S., Ueda, T.,
Behavior of liquid and flooding in countercurrent two-phase flow - part 1: Flow in circular tubes,
Int. J. Multiphase Flow, Vol. 3 , pp 517 - 532

/11/ Grolmes, M.A., Lambert, G.A., Fauske,H.K.
Flooding in vertical tubes,
ICHEME Symposium Series No. 38 A4, 1974

/12/ Dukler, A.E., Chopra, A., Moalim, D., Semiat, R.,
Two-Phase Interactions in countercurrent flow,
Annual Report Nov. 1977 - Oct. 1978,
University of Houston, NUREG/CR-0669

/13/ Taitel, Y., Barnea, D., Dukler, A.E.,
A film mo-el for the prediction of flooding and flow reversal for gas-liquid flow in vertical tubes,
Int. J. Multiphase Flow Vol. 8, No. 1, pp. 1-10, 1982

/14/ Shearer and Davidson,
The investigation of a standing wave due to gas blowing upwards over a liquid film, its relation to flooding in wetted wall columns,
J. Fluid Mechanics Vol. 22, part 2, pp 321-335, 1965

/15/ Cetinbadakler, A.G., Jameson, G.I.,
The mechanism of flooding in vertical countercurrent two-phase flow,
Chem. Eng. Sci. Vol. 24, pp 1669-1680, 1969

/16/ Imura, H., Kusuda, H., Fumatsa, S.,
Flooding velocity in a countercurrent
annular two-phase flow,
Chem. Eng. Sci. Vol. 32 pp 79-87, 1969

/17/ Richter, H.I.,
Flooding in tubes and annuli
Int. Journal Multiphase Flow, Vol. 7
No. 6 pp 647-658, 1981

/18/ Zvirin, Y., Duffey, R.B., Sun, K.H.,
On the derivation of a countercurrent
flooding theory,
Winter Annual Meeeting if the ASME, New
York, 1979

/19/ Wallis, G.B., Jing Tzong Kuo
The behaior of gas-liquid interfaces
in vertical tubes.
Int. J. Multiphase Flow, Vol. 2,
pp 521-536, Pergamon, 1976

/20/ Naitoh, M., Chino, K., Kawabe, R.,
Restrictive Effect of Ascending Steam
on falling water during Top Spray
Emergency Core Cooling.
Journal of Nuclear Science and
Technologie
15 (11) pp 806-815 Nov. 1978

/21/ Liu, C.P., Tien, C.L.,
A review on gas-liquid countercurrent
flow through multiple path.
no. ref., Dep. of Mech. Eng., Universi-
ty of California, Berkeley, USA